arXiv:2104.09605v3 [physics.ins-det] 26 Apr 2021

Prepared for submission to JINST

A D_2O detector for flux normalization of a pion decay-at-rest neutrino source

COHERENT collaboration

D. Akimov,[a] **P. An,**[b,c] **C. Awe,**[b,c] **P.S. Barbeau,**[b,c] **B. Becker,**[d] **V. Belov ,**[e,a] **I. Bernardi,**[d] **M.A. Blackston,**[f] **L. Blokland,**[d] **A. Bolozdynya,**[a] **B. Cabrera-Palmer,**[g] **D. Chernyak,**[h] **E. Conley,**[b] **J. Daughhetee,**[d,f] **E. Day,**[i] **J. Detwiler,**[j] **K. Ding,**[h] **M.W. Durand,**[j] **Y. Efremenko,**[d,f] **S.R. Elliott,**[k] **L. Fabris,**[f] **M. Febbraro,**[f] **A. Gallo Rosso,**[l] **A. Galindo-Uribarri,**[f,d] **M.P. Green ,**[c,f,m] **M.R. Heath,**[f] **S. Hedges,**[b,c] **D. Hoang,**[i] **M. Hughes,**[n] **T. Johnson,**[b,c] **A. Khromov,**[a] **A. Konovalov,**[a,e] **J. Koros,**[c,1] **E. Kozlova,**[a,e] **A. Kumpan,**[a] **L. Li,**[b,c] **J.M. Link,**[o] **J. Liu,**[h] **D.M. Markoff,**[p,c] **K. Mann,**[m] **P.E. Mueller,**[f] **J. Newby,**[f] **D.S. Parno,**[i] **S. Penttila,**[f] **D. Pershey,**[b] **R. Rapp,**[i] **H. Ray,**[q] **J. Raybern,**[b] **O. Razuvaeva,**[a,e] **D. Reyna,**[g] **G.C. Rich,**[c] **J. Ross,**[p,c] **D. Rudik,**[a] **J. Runge,**[b,c] **D.J. Salvat,**[n] **A.M. Salyapongse,**[i] **K. Scholberg,**[b] **A. Shakirov,**[a] **G. Simakov,**[a,e] **G. Sinev,**[b,2] **W.M. Snow,**[n] **V. Sosnovstsev,**[a] **B. Suh,**[n] **R. Tayloe,**[n] **K. Tellez-Giron-Flores,**[o] **I. Tolstukhin,**[n,3] **E. Ujah,**[p,c] **J. Vanderwerp,**[n] **R.L. Varner,**[f] **C.J. Virtue,**[l] **G. Visser,**[n] **C. Wiseman,**[j] **T. Wongjirad,**[r] **Y.-R. Yen,**[i] **J. Yoo,**[s,t] **C.-H. Yu,**[f] **J. Zettlemoyer**[n,4]

[a] *National Research Nuclear University MEPhI (Moscow Engineering Physics Institute), Moscow, 115409, Russian Federation*

[b] *Department of Physics, Duke University, Durham, NC, 27708, USA*

[c] *Triangle Universities Nuclear Laboratory, Durham, NC, 27708, USA*

[d] *Department of Physics and Astronomy, University of Tennessee, Knoxville, TN, 37996, USA*

[e] *Institute for Theoretical and Experimental Physics named by A.I. Alikhanov of National Research Centre "Kurchatov Institute", Moscow, 117218, Russian Federation*

[f] *Oak Ridge National Laboratory, Oak Ridge, TN, 37831, USA*

[g] *Sandia National Laboratories, Livermore, CA, 94550, USA*

[h] *Physics Department, University of South Dakota, Vermillion, SD, 57069, USA*

[i] *Department of Physics, Carnegie Mellon University, Pittsburgh, PA, 15213, USA*

[j] *Center for Experimental Nuclear Physics and Astrophysics & Department of Physics, University of Washington, Seattle, WA, 98195, USA*

[k] *Los Alamos National Laboratory, Los Alamos, NM, 87545, USA*

[l] *Department of Physics, Laurentian University, Sudbury, Ontario, P3E 2C6, Canada*

[m] *Department of Physics, North Carolina State University, Raleigh, NC, 27695, USA*

[n] *Department of Physics, Indiana University, Bloomington, IN, 47405, USA*

[o] *Center for Neutrino Physics, Virginia Tech, Blacksburg, VA, 24061, USA*

[p] *Department of Mathematics and Physics, North Carolina Central University, Durham, NC, 27707, USA*

[q] *Department of Physics, University of Florida, Gainesville, FL, 32611, USA*

[r] *Department of Physics and Astronomy, Tufts University, Medford, MA, 02155, USA*

[s] *Department of Physics, Korea Advanced Institute of Science and Technology, Daejeon, 34141, Republic of Korea*

[t] *Center for Axion and Precision Physics Research (CAPP) at Institute for Basic Science (IBS), Daejeon, 34141, Republic of Korea*

E-mail: heathmr@ornl.gov

[1] Now at: Department of Physics, University of Notre Dame, IN, 46556, USA

[2] Now at: South Dakota School of Mines and Technology, Rapid City, SD, 57701, USA

[3] Now at: Argonne National Laboratory, Argonne, IL, 60439, USA

[4] Now at: Fermi National Accelerator Laboratory, Batavia, IL, 60510, USA

ABSTRACT: We report on the technical design and expected performance of a 592 kg heavy-water-Cherenkov detector to measure the absolute neutrino flux from the pion-decay-at-rest neutrino source at the Spallation Neutron Source (SNS) at Oak Ridge National Laboratory (ORNL). The detector will be located roughly 20 m from the SNS target and will measure the neutrino flux with better than 5 % statistical uncertainty in 2 years. This heavy-water detector will serve as the first module of a two-module detector system to ultimately measure the neutrino flux to 2–3 % at both the First Target Station and the planned Second Target Station of the SNS. This detector will significantly reduce a dominant systematic uncertainty for neutrino cross-section measurements at the SNS, increasing the sensitivity of searches for new physics.

KEYWORDS: Cherenkov and transition radiation, Cherenkov detectors, Neutrino detectors

Contents

1 Introduction **1**

2 Neutrinos from the Spallation Neutron Source **3**

3 Neutrino Interactions on D_2O **4**

4 Fundamentals of D_2O Detector Design **4**

5 Performance Goals **6**

6 Signal and Background Predictions **7**
6.1 Signal Prediction 7
6.2 Background Predictions 8

7 Estimated Rates and Sensitivity **10**

8 Potential Physics Impact **11**

9 Conclusions **13**

1 Introduction

Coherent elastic neutrino-nucleus scattering (CEvNS) is a type of neutral-current neutrino scattering that was predicted in 1974 [1, 2] and experimentally observed in 2017 [3] by the COHERENT experiment. In CEvNS, a neutrino scatters coherently from an entire nucleus rather than from an individual nucleon, resulting in a large boost to the cross section. With a cross section on the order of 1×10^{-39} cm^2, the CEvNS interaction is roughly 100 times more likely to occur than other neutrino interactions at a few tens of MeV for heavy nuclei, so CEvNS-sensitive neutrino detectors can be made quite compact. Unfortunately, the CEvNS process is extremely challenging to detect because of the tiny nuclear recoil energies involved. Nonetheless, COHERENT's initial result on CsI was followed by a positive observation on argon [4].

The Standard Model provides a very clean and direct prediction of the CEvNS cross section [5]. A precise measurement of the CEvNS cross section can thus be used to search for new physics beyond the Standard Model. For example, the neutrino magnetic moment [6–9] and the neutrino

[5]This manuscript has been authored by UT-Battelle, LLC, under contract DE-AC05-00OR22725 with the US Department of Energy (DOE). The US government retains and the publisher, by accepting the article for publication, acknowledges that the US government retains a nonexclusive, paid-up, irrevocable, worldwide license to publish or reproduce the published form of this manuscript, or allow others to do so, for US government purposes. DOE will provide public access to these results of federally sponsored research in accordance with the DOE Public Access Plan (http://energy.gov/downloads/doe-public-access-plan).

charge radius [10] will affect the CEvNS cross section. COHERENT's first CEvNS measurement has already been used to set competitive bounds on the neutrino charge radius [11]. Since it is a neutral-current process, CEvNS also provides an attractive possible strategy for an oscillation-based sterile-neutrino search [12, 13]. Finally, the CEvNS cross section is also sensitive to so-called non-standard neutrino interactions (NSI) [8, 14–17], beyond-Standard Model interactions of neutrinos and quarks. Through this sensitivity to NSI, CEvNS measurements can help to resolve degeneracies in the mass-ordering determination from long-baseline neutrino experiments such as DUNE [18–21].

Even in the absence of new physics, CEvNS measurements will help untangle the low-energy nuclear recoil responses of various detector technologies, providing valuable calibration input for WIMP dark-matter searches with similar technologies. As the interaction and detector response are better characterized, CEvNS will become a possible tool for compact nuclear nonproliferation monitors. Unlike inverse beta decay, it is sensitive to low-energy capture antineutrinos from uranium breeder blankets [22], as CEvNS is sensitive to neutrinos below the inverse beta decay threshold. Finally, precision measurements of CEvNS cross sections will improve our understanding of the target nuclei through measurements of the neutron radius [23–26], which is a crucial input for our understanding of neutron-rich matter, from exotic nuclei to neutron stars.

The COHERENT experiment is located in "Neutrino Alley," a basement corridor roughly 20 m from the pion-decay-at-rest neutrino source at the Spallation Neutron Source (SNS), a US Department of Energy (DOE) User Facility located at Oak Ridge National Laboratory (ORNL). COHERENT is establishing a long-term program to study the CEvNS interaction on various nuclei to confirm the proportionality of the cross section to the number of neutrons squared (N^2), and to use CEvNS for some of the physics measurements mentioned above. In addition to the CEvNS measurements with CsI and argon made to date [3, 4], the collaboration is deploying additional detectors to search for CEvNS in multiple materials (NaI and germanium) to further test the N^2 dependence, as well as measuring the cross sections of other neutrino interactions of particular relevance to neutrino and supernova physics [27]. For example, the charged-current cross section $^{127}\mathrm{I}(\nu_e, \mathrm{e}^-)^{127}\mathrm{Xe}^*$ is under study, along with neutrino-induced neutron emission of lead and iron. In addition, charged-current neutrino interactions with argon, relevant for interpreting a DUNE supernova signature [28], will be studied with a tonne-scale liquid argon detector in the future [27].

For the current COHERENT results [3, 4], one of the dominant systematic uncertainties is due to the estimated 10 % uncertainty on the neutrino flux from the SNS target. This uncertainty arises from comparisons between model predictions and the sparse available world data. To that end, a 592 kg heavy-water Cherenkov detector has been designed to operate in Neutrino Alley. This detector will make use of the well-understood ν_e + d interaction cross section [29–31] to greatly reduce the uncertainty on the SNS neutrino flux.

This paper describes the design and expected performance of such a heavy-water detector. Section 2 describes the SNS neutrino source. Section 3 describes the current status of the relevant theoretical D_2O neutrino cross sections. Section 4 describes the design of the detector. Section 5 covers the expected detector performance. Sections 6 and 7 cover the expected signals and backgrounds and their predicted rates. Finally, Section 8 discusses the expected physics impacts of such a heavy-water detector operating at the SNS.

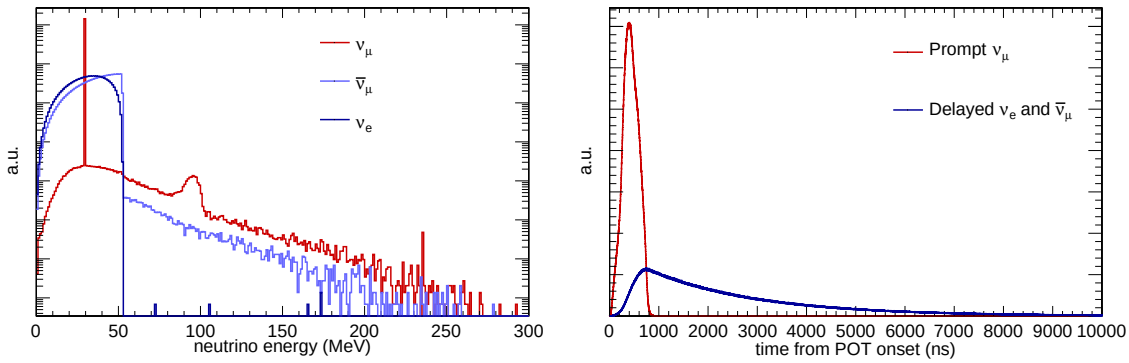

Figure 1: Simulated energy (left) and time (right) spectra for neutrinos from a stopped-pion neutrino source like the ORNL SNS.

2 Neutrinos from the Spallation Neutron Source

The SNS is a user facility that operates a 1.4 MW proton beam. Neutrons at the SNS are produced by bunches of roughly 1 GeV protons impinging on a thick liquid-mercury target. In addition to the neutrons produced at the SNS, copious charged pions are also produced in the target, with approximately 0.09 π^+ created for every proton on target (POT) [32]. Approximately 99 % of the π^- are captured in the thick mercury target, while the π^+ stop and decay at rest in the target. These decaying pions ultimately produce three different neutrinos for each pion decay, with an energy spectrum extending up to 53 MeV (Figure 1):

$$\pi^+ \rightarrow \nu_\mu + \mu^+; \qquad \mu^+ \rightarrow \bar{\nu}_\mu + \nu_e + e^+. \tag{2.1}$$

This results in an approximate neutrino flux of 4.3×10^7 neutrinos/cm^2/s at a distance of 20 m [27]. Owing to the short π^+ lifetime (26 ns), the ν_μ are produced roughly in tandem with the beam pulse and follow the protons-on-target time profile. The $\bar{\nu}_\mu$ and ν_e are delayed according to the lifetime of the μ^+ decay (2.2 µs) as seen in Figure 1.

These neutrinos are ideal for a CEvNS experiment. The relatively large neutrino energies produce larger nuclear-recoil energies than do reactor-produced neutrinos, although very low detector thresholds are still required. In addition, because of the underlying timing structure of the SNS proton beam (60 Hz bursts with full width at half maximum of 350 ns each), neutrinos arrive at the COHERENT detectors in well-defined pulses. This timing permits neutrino-flavor separation as well as the precise subtraction of steady-state backgrounds.

The neutrino flux from the SNS target was estimated with a GEANT4 [33–35] simulation, which relies on the Bertini intranuclear cascade model of hadronic interactions [36] to predict the intensity of pion production in the target based on the characteristics of the proton beam [32]. However, the pion-production cross section for 1 GeV protons on a mercury target has never been measured. Furthermore, a full accounting of charged-pion production in the target requires knowledge of pion-production cross-sections at lower energies, as protons rapidly lose energy to ionization interactions once they enter the SNS target, and at all production angles. Uncertainties in the model predictions give rise to an estimated 10 % uncertainty on the neutrino flux, the second-largest systematic in

COHERENT's published result on CsI [3] and the largest on the full CsI result, following an improved determination of the CsI quenching factor by the COHERENT collaboration [37, 38]. It is also the largest systematic uncertainty in our first result on argon [4] and is the dominant systematic uncertainty shared across all COHERENT neutrino detectors. Reducing the neutrino-flux uncertainty will benefit cross-section measurements, and the corresponding physics impact, for all COHERENT detectors.

To reduce this systematic, a 592 kg heavy-water detector has been designed, taking advantage of the current 2–3 % theoretical uncertainty (Section 3) on the charged-current deuteron cross section to measure the neutrino flux directly.

3 Neutrino Interactions on D_2O

Many neutrino-interaction cross sections of nuclei in the energy range relevant for pion-decay-at-rest neutrinos (a few tens of MeV) are not well constrained experimentally [39]. The charged-current cross section on deuterium is one of the best-understood interactions [40–45]. This cross section has also benefited from extensive theoretical studies using a variety of tools, including potential models, pionless effective field theory, and the EFT* approach of combining potential-model wave functions with transition operators from chiral perturbation theory [46].

Based on these theoretical studies, the ν_e + d interaction cross section is constrained to 2–3 % simply by the agreement between unconstrained calculations using these approaches [29, 30]. This uncertainty envelope may be further reduced by experimental constraints on the axial exchange-current operator [30, 46, 47], and active theoretical progress is continuing [30, 31]. Sensitivity calculations are ongoing, but we anticipate that with 592 kg of D_2O, we can achieve a statistical precision of better than 5 % in 2 years of running time at the SNS, as discussed below, approaching the current theoretical uncertainty of the ν_e + d cross section.

In addition to charged-current deuteron scattering, a heavy-water detector can also study the $\nu_e + {}^{16}\mathrm{O} \longrightarrow \mathrm{e}^- + {}^{16}\mathrm{F}^*$ charged-current interaction. Such a measurement would provide valuable cross-section information for supernova detection in existing and future large water Cherenkov detectors [48, 49].

4 Fundamentals of D_2O Detector Design

A 592 kg heavy-water detector has been designed to fit alongside the various neutrino detectors present at the SNS in Neutrino Alley (Figure 2). It will both provide an initial measurement of the neutrino flux from the SNS and study beam-related backgrounds, light-collection efficiency, and event reconstruction in situ. Note that the heavy-water detector will operate in a different energy regime from CEvNS detectors in Neutrino Alley, searching for tens-of-MeV electrons. This detector will serve as the first stage of a two-module detector that will reduce one of the leading COHERENT uncertainties by a factor of 2 or better. Improving this flux-normalization uncertainty is a critical milestone on the path to precision CEvNS measurements at the SNS.

The D_2O detector will be deployed roughly 90° off-axis and approximately 20 m from the SNS target (Figure 2). At this location, there is very little contribution from decay-in-flight neutrinos (less than 1 % of the total neutrino spectrum), which are boosted forward. Since Neutrino Alley is

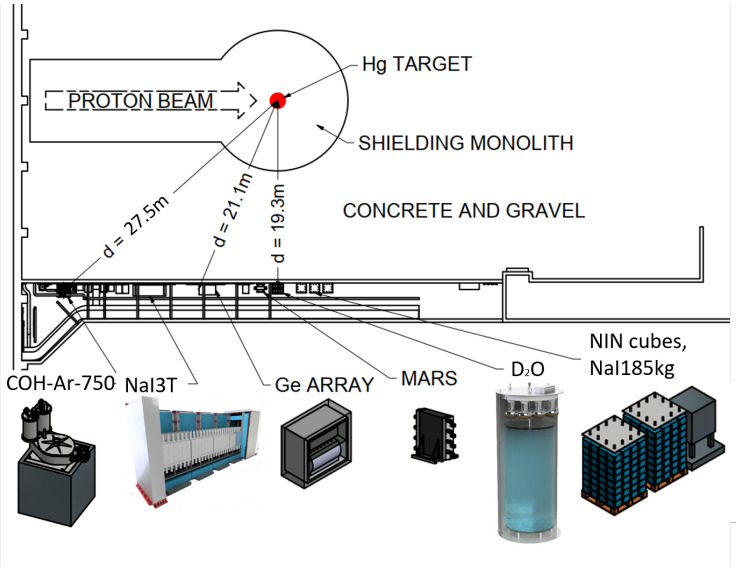

Figure 2: Planned near-future deployment of COHERENT detectors in Neutrino Alley at the SNS. The precise siting of the Multiplicity And Recoil Spectrometer (MARS) neutron monitoring detector can readily be changed based on the needs of the collaboration.

a basement corridor with required egress routes, there is no space for photomultiplier tubes (PMTs) to be mounted perpendicular to the hallway walls. Even in that orientation, the space constraints in Neutrino Alley, along with passive and active shielding requirements for the detector, limit the possible width of the detector. To satisfy these constraints with a cost-effective system, the detector geometry consists of an upright cylinder, with 592 kg of heavy water contained inside a clear acrylic vessel 70 cm in diameter and 140 cm tall (Figure 3). The acrylic vessel is 0.6 cm thick on the sides with 2.54 cm thick end caps.

Within this well-defined volume, electrons from the primary reaction

$$\nu_e + \mathrm{d} \longrightarrow \mathrm{p} + \mathrm{p} + \mathrm{e}^- \tag{4.1}$$

produce Cherenkov radiation, which passes through the acrylic container into an outer volume of H_2O with a thickness of 10 cm, contained within a 0.64 cm thick steel tank. Electrons that escape the central volume will still produce Cherenkov light in this "tail-catcher" region, allowing a more complete integration of the total electron energy. Twelve Hamamatsu R5912-100 8 inch PMTs, immersed in the H_2O, will view the fiducial volume from above.

To compensate for the absence of 4π photocathode coverage, the inner walls of the steel tank will be covered in reflective Tyvek®. Even commercially available Tyvek has favorable optical properties [50]. With this reflector, light collection within the D_2O volume will remain relatively uniform, but well-defined Cherenkov rings from, e.g., cosmic-ray backgrounds cannot be reconstructed. Energy and timing cuts will therefore be the primary means of background discrimination.

Outside the steel tank that supports the PMTs and encloses the tail catcher, 2.54 cm of lead shielding and two layers of 2.54 cm plastic scintillator panels read out via wavelength-shifting

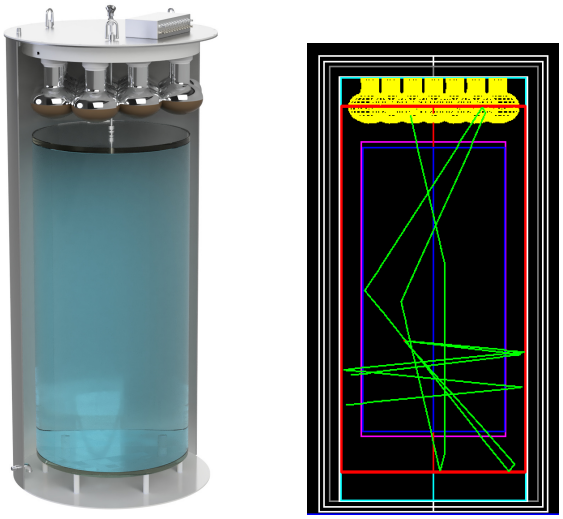

Figure 3: *Left:* Engineering drawing of the detector, showing the fiducial volume of D_2O in blue, along with the photomultiplier tubes, inside the steel tank. *Right:* Side view of a simulated event. A small number of Cherenkov-photon paths generated by an electron are shown in green. Also visible is the Tyvek® reflector (red), steel vessel (cyan), Pb shielding (gray), and two-layer muon veto (white).

fibers [50] will mitigate external backgrounds due to beam-related neutrons, radioactivity in the hall, and cosmic rays. Additional detector designs are under consideration to increase the photon yield pending the availability of additional PMTs.

5 Performance Goals

The energy calibration will be established with Michel electrons from the decay at rest of cosmic-ray muons that stop in the fiducial volume. These electrons have a well-characterized energy spectrum extending to about 53 MeV [51, 52], which overlaps with the electron energy spectrum from the ν_e + d interaction. This technique is used by many collaborations; see for example Abe et al. [48]. A system of light-emitting diode flashers, mounted inside the steel tank, will monitor the homogeneity and stability of the detector response. This system will provide the capability to incorporate an understanding of photomultiplier gains and the transparency of the water and the acrylic volumes into the modeled detector response.

To evaluate the expected performance of the heavy-water detector, a GEANT4 simulation of the detector geometry discussed in Section 4 was developed. The simulation places the detector inside a mock-up of Neutrino Alley, including the 2.4 m of concrete overburden for cosmic-ray background predictions.

This detector simulation was used to predict both the expected energy resolution and the detected photon yield, as well as to evaluate the predicted spectra from various signals and backgrounds of interest, as discussed in Section 6. In the simulation, the reflectivity of the Tyvek coating was

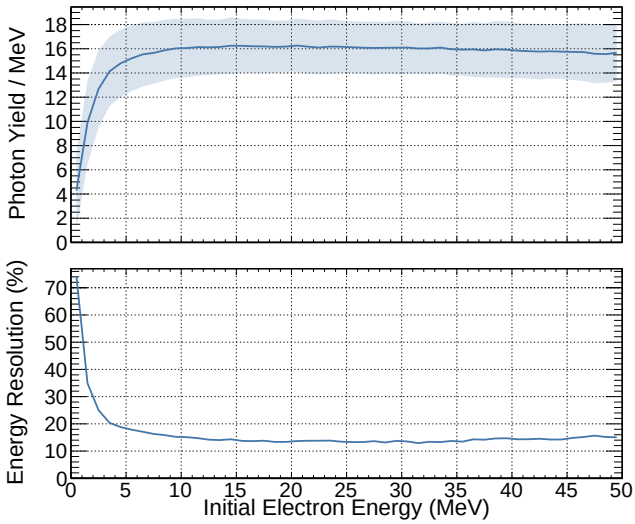

Figure 4: Expected detected photon yield (top) and fractional energy resolution (σ/E_i, bottom) for electrons, as a function of initial electron energy. The top panel shows a statistical $\pm 1\sigma$ band around the mean.

assumed to be 97 % [53]. The wavelength dependence of the PMT quantum efficiency [54] was also incorporated.

Figure 4 shows the expected energy resolution and detected photon yield of the heavy-water detector. For this GEANT4 simulation study, electrons (representing the detectable product of charged-current interactions) were generated isotropically within the fiducial volume, with known initial energies ranging uniformly from 1–55 MeV. The energy was then reconstructed based on the number of photoelectrons recorded by the simulated high-quantum-efficiency R5912-100 PMTs. Within a narrow range of initial energies, the response peak was fit to a Gaussian with an exponential tail [55], and the standard deviation was taken as the energy resolution. An expected photon yield of 16 photons/MeV should provide sufficient energy resolution (roughly 15 % above 30 MeV) to separate the charged-current ν_e + d signal from the expected backgrounds discussed below. While the detected photon yield was found to depend on the assumed reflectivity of the Tyvek reflector, the assumed reflectivity was found to have a minimal effect on the reconstructed signal and background spectra.

6 Signal and Background Predictions

6.1 Signal Prediction

The GEANT4 simulation described in Section 5 was used to predict the observed ν_e + d signal. The charged-current ν_e + d cross section [56, 57], see Figure 5, was folded with the estimated neutrino flux [32] at the location of the D_2O detector to form the true charged-current-induced electron spectrum (Figure 6). The response matrix obtained in Section 5 was then folded with this distribution to produce the expected observed spectrum after running for 2 SNS-years (where an SNS-year is defined as 5000 hours of operation at 1.4 MW) as seen in Figure 7.

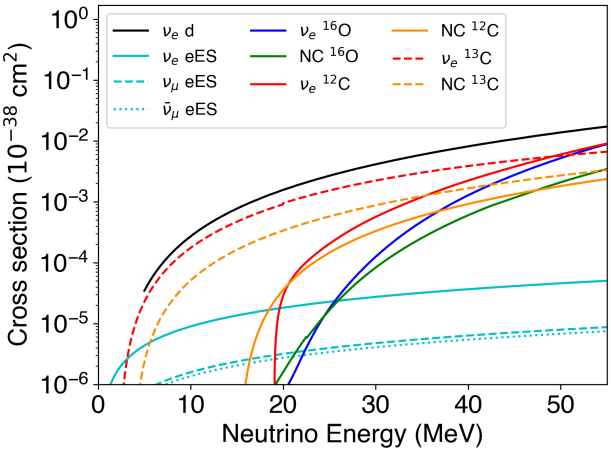

Figure 5: Cross sections for neutrino interactions with heavy-water detector materials. 'eES' refers to neutrino-electron elastic scattering.

6.2 Background Predictions

While beam-related neutrons are a significant background for CEvNS searches at the SNS, they are not expected to be a major background for the heavy-water detector, as their interactions produce signals below the Cherenkov threshold in D_2O. Data from other COHERENT detectors do not indicate the presence of a significant delayed neutron flux (arriving after the 800 ns SNS beam pulse) in Neutrino Alley [3, 4, 58]. This finding further mitigates any potential background from beam-related neutrons, as the ν_e neutrino signal of interest will arrive delayed relative to the beam time profile. Any potential background from delayed thermal neutron captures in the tail-catcher region will be removed with an energy threshold. Nevertheless, the beam-related neutron flux will be monitored by the existing Multiplicity And Recoil Spectrometer (MARS) detector [59] in Neutrino Alley.

Neutrino-induced backgrounds are estimated using the SNOwGLobES [60] package, using cross sections shown in Fig. 5. Charged- and neutral-current interactions with oxygen can occur in the fiducial volume or in the tail-catcher region. The ν_e on ^{16}O interaction [61] is also a signal of interest, see Section 3, and may also be measured with a separate H_2O run of the detector. The neutral-current excitation of oxygen [62] can produce deexcitation gammas, but with energies less than roughly 8 MeV, and for which Compton scatters produce yet smaller event energies—so these should be a negligible background.

Although charged- and neutral-current interactions with the carbon atoms [63, 64] in the acrylic are possible, the rates are negligible because of the low acrylic mass in the detector. Any charged-current events from carbon that do occur may also be removed with an energy-threshold cut. Elastic scatters of neutrinos on electrons occur with well-known cross sections, but are a tiny contribution to the event rate. Interaction rates as a function of neutrino energy are shown in Fig. 6.

As the dominant neutrino-produced beam-related background, the true charged-current-on-O energy spectrum was folded with the response matrix formed from the simulation discussed in Section 5 to produce the spectrum shown in Figure 7. Because the energy spectrum of electrons produced from charged-current interactions with oxygen peaks approximately 18 MeV lower in

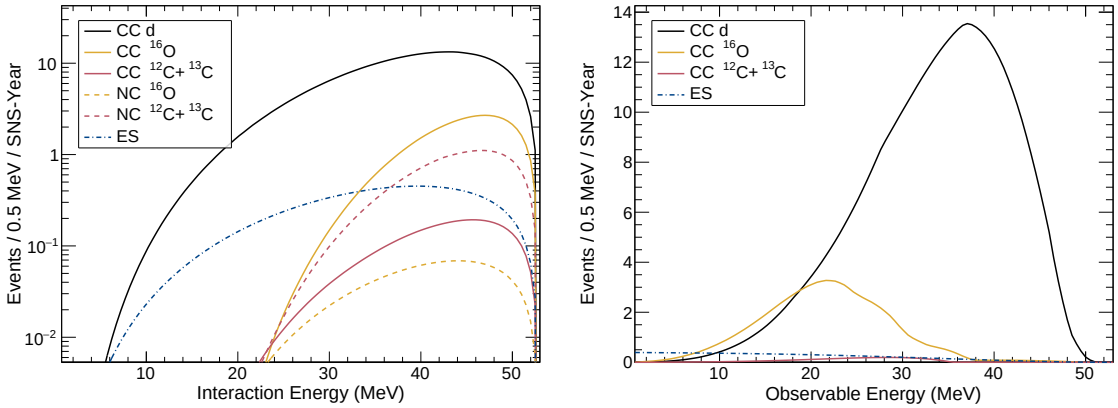

Figure 6: *Left*: Estimated count rates for various neutrino interactions per SNS beam-year as predicted by SNOwGLoBES [60], as a function of neutrino energy. Note that neutral-current interactions result in deexcitation gammas, for which only a fraction of the energy will be observed. *Right*: Expected count rates for charged-current neutrino interactions in the D_2O detector for dominant interactions. Smearing from imperfect energy resolution was not included in this plot. Smeared spectra are presented in Figure 7.

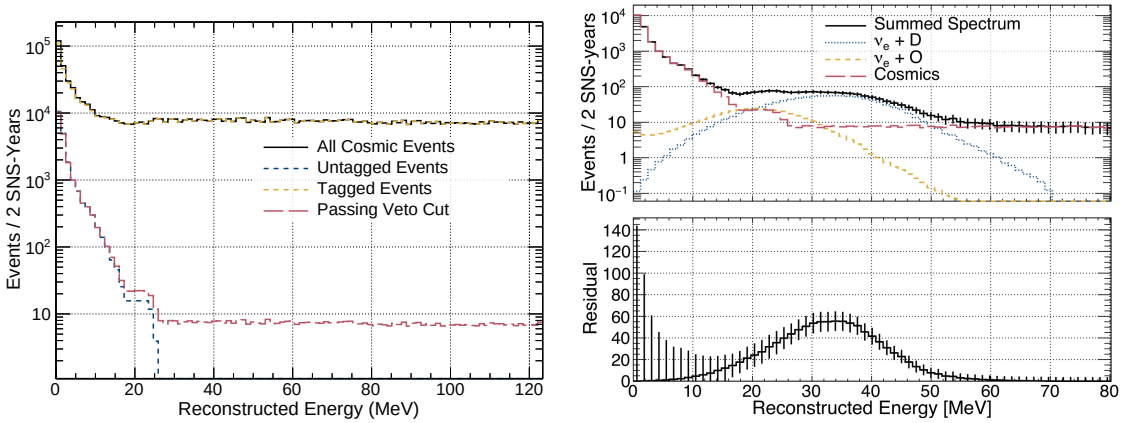

Figure 7: Expected event rates in the heavy-water detector. *Left:* Expected background from cosmic rays as predicted with the CRY [65] module and simulated with the GEANT4 simulation described in Section 5, with and without a muon veto as discussed in Section 6.2. *Top right*: Simulated signal and background energy spectra as reconstructed with the heavy-water detector. *Bottom right*: The background-subtracted ν_e + d spectrum with statistical errors. As discussed in the text, an energy threshold above roughly 20 MeV will remove most of the background contamination from the expected deuteron signal. Smearing from imperfect energy resolution is included here.

energy, they can be removed with an energy threshold as seen in Figs. 6 and 7.

The most significant expected background is cosmic-ray products that lie above the Cherenkov threshold in D_2O, especially given the expected lack of angular reconstruction capabilities of the detector. The CRY [65] cosmic-ray-generator package was used as input to the GEANT4 simulation described in Section 5 to predict the cosmic-ray-induced backgrounds for the heavy-water detector. Cosmic rays were generated at the surface and transported through the 2.4 m of concrete overburden above Neutrino Alley.

There are two classes of cosmic-ray-induced background events: tagged and untagged. Tagged events are those that deposit more than 5 MeV in the muon veto. With the high light-collection efficiencies possible in veto panels [50] and good hermiticity, muons will be tagged with an efficiency close to 99.9 %. Even with the beam duty factor (6×10^{-4}), this high efficiency is needed because of the shallow overburden in Neutrino Alley. As seen in Figure 7, these backgrounds, and in particular higher-energy cosmic rays with a reconstructed energy of $\gtrsim$ 20 MeV, can be largely removed with the inclusion of a two-layer muon veto. Deadtime concerns due to the cosmic-ray flux are anticipated to be on the order of a few percent based on the measured muon flux in Neutrino Alley.

7 Estimated Rates and Sensitivity

The results from the GEANT4 simulations described in Section 5 and 6 were used to predict the rates from the charged-current ν_e + d signal and the dominant expected background spectra and rates. As seen in Figure 6 and Figure 7, most expected backgrounds reside at a lower energy than the charged-current deuterium signal. This result provides the opportunity to minimize the background contamination of the signal with an energy acceptance window. While a full likelihood fit would maximize the expected sensitivity to the deuterium signal, a simple one-binned counting experiment of events within an energy window is sufficient to conservatively estimate the statistical precision possible with the heavy-water detector.

The statistical precision is given by

$$\alpha \equiv \frac{\sigma}{N} = \frac{\sqrt{N + 2B}}{N}, \tag{7.1}$$

where σ is the statistical uncertainty of the number of signal events N, and B is the expected number of background events. In this case, an additional scale factor of 2 in the numerator follows the pessimistic assumption that the backgrounds will not be well measured. In reality, the cosmic background will be well measured between proton pulses, reducing the factor of 2 and increasing the signal significance. The background from oxygen charged-current events will occur in tandem with the beam and will need either to be measured with a separate H_2O fill of the detector or to be modeled by simulation and included in a simultaneous fit.

The expected spectra due to the charged-current-deuterium signal and the dominant backgrounds may be seen in Figure 7. An optimal energy window was found to minimize the statistical uncertainty of the background-subtracted number of signal events. For the heavy-water detector, an energy acceptance window of greater than 22 MeV and less than 68 MeV minimized the statistical uncertainty of a one-bin counting experiment, with an expected precision of 4.7 % in 2 SNS-years of running time, as seen in Figure 8.

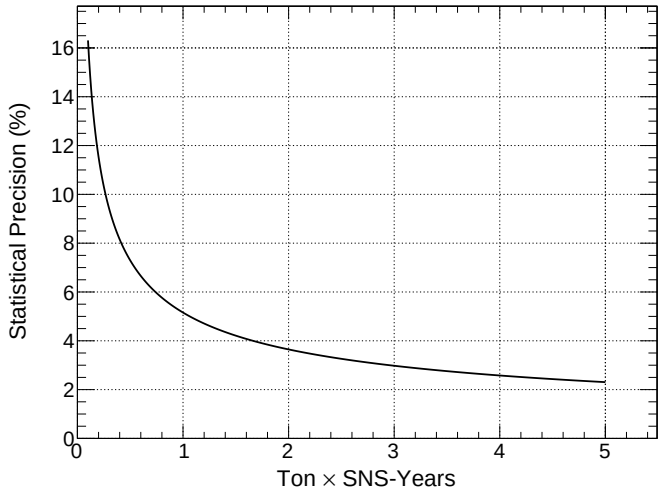

Figure 8: Expected statistical uncertainty of the number of charged-current-deuterium events as a function of mass and time. The SNS operates for 5000 h every year at 1.4 MW.

Table 1 summarizes the expected event rates in the single-module heavy-water detector following 2 SNS-years of running both with and without the energy cut discussed earlier. As seen in the table, a total of 1070 signal events are expected in 2 years of run time, with 910 of those events occurring within the optimal energy range for a counting experiment.

8 Potential Physics Impact

The Standard Model predicts that the CEvNS cross section is approximately proportional to the square of the number of neutrons in the nucleus ($\propto N^2$). One of the main goals of the COHERENT experiment is to verify this N^2 prediction by using a suite of detectors with different nuclei. In such a comparison, the SNS neutrino flux represents a common factor among the detectors and drops out in the ratio. However, the neutrino flux is a significant source of uncertainty for any measurement involving an absolute cross section.

	Total Events	**Events in Region of Interest**
$\nu_e + d$	1070	910
$\nu_e + O$	390	160
Cosmics	21150	315

Table 1: Expected signal and major-background event rates in the single-module heavy-water detector following 2 SNS-years of running at 1.4 MW and a duty factor of 6×10^{-4}. Energy, timing, and veto cuts will remove much of the backgrounds for the ν_e + d signal as discussed in the text. An optimal energy region of interest from 22–68 MeV will produce an expected statistical precision for a simple event-counting analysis of 4.7 %.

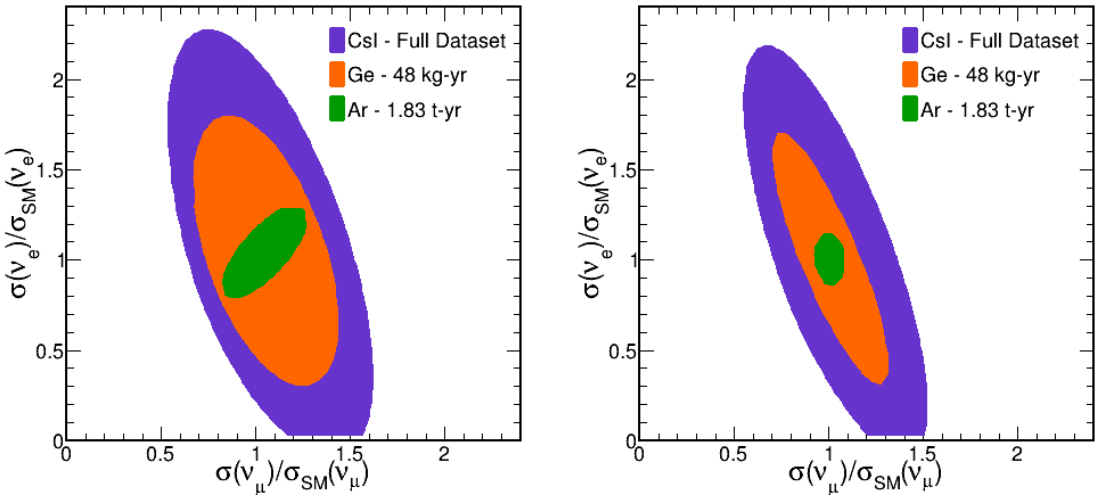

Figure 9: Predicted sensitivity to deviations from the Standard Model CEvNS cross section for ν_μ and ν_e neutrinos. The "CsI–Full Dataset" regions correspond to the full CsI dataset from the COHERENT experiment with roughly twice the accumulated statistics of the initial result [37]. *Left*: Current 10 % neutrino-flux uncertainty. *Right*: Allowed regions assuming the SNS neutrino flux is measured with a precision matching the current 3 % theoretical uncertainty of the ν_e + d cross section.

There are multiple physics results that can be affected by a precise flux normalization. Let us illustrate that with one example. As CEvNS is a neutral-current process, the cross section is flavor-independent in the Standard Model, with small differences from radiative corrections [66–68]. So-called non-standard neutrino interactions (NSI), which are crucial to understanding the mass-ordering determination from long-baseline neutrino-oscillation experiments [18–20], can manifest as a flavor dependence of the CEvNS cross section. The precise timing of the SNS beam allows for flavor separation of the incident neutrinos, providing an opportunity to search for a flavor dependence of the CEvNS cross section.

Taking advantage of this flavor separation, Figure 9 shows the expected constraints on the ν_μ and the ν_e CEvNS cross sections relative to the Standard Model predictions. Shown in the left panel are the expected constraints on the CEvNS cross section for electron- and muon-flavored neutrinos relative to their Standard-Model predictions with the current 10 % uncertainty of the incident neutrino flux. The right panel shows the improved constraints assuming the flux uncertainty can be reduced to the theoretical 3 % uncertainty of the ν_e + d cross section following deployment of the second heavy-water detector module at the SNS, as well as the next generation of COHERENT CEvNS detectors discussed in Section 1. The improved knowledge of the neutrino flux enabled by a heavy-water detector at the SNS would reduce the allowed parameter space by roughly a factor of 2. Any deviations from the Standard Model prediction, and in particular any flavor dependence of the cross section, would be an indication of physics beyond the Standard Model.

9 Conclusions

One of the dominant systematic uncertainties for neutrino detectors operating at the pion decay-at-rest neutrino source at the ORNL SNS is the 10 % uncertainty of the incident neutrino flux. A heavy-water Cherenkov detector has been designed to capitalize on the small (2–3 %) theoretical uncertainty of the charged-current ν_e + d interaction. The detector will fit in the available space within Neutrino Alley and make a direct measurement of the SNS neutrino flux with a statistical uncertainty of 4.7 % in 2 SNS-years. This detector is the first of a two-module design that will enable the COHERENT experiment to normalize the neutrino flux from the SNS, ultimately to 3 % precision, allowing a corresponding increase in sensitivity to new physics beyond the Standard Model.

As a case study in the increased physics sensitivity capable of being probed with a reduced neutrino flux uncertainty at the SNS, the allowed region for a flavor dependence of the CEvNS cross section was studied. The allowed region was shown to shrink by roughly a factor of 2, assuming a reduction in the flux uncertainty from the current 10 % to an uncertainty of 3 %, matching the theoretical uncertainty of the ν_e + d cross section. Following this initial program to calibrate the neutrino flux for 1 GeV protons at the SNS, the detector will also be used to calibrate the flux at 1.3 GeV following the SNS Proton Power Upgrade [69]. It will later be moved to the ORNL SNS Second Target Station [70] to further support future neutrino efforts at the SNS.

Acknowledgments

The COHERENT collaboration acknowledges the resources generously provided by the Spallation Neutron Source, a DOE Office of Science User Facility operated by the Oak Ridge National Laboratory. This work was supported by the US Department of Energy (DOE), Office of Science, Office of High Energy Physics and Office of Nuclear Physics; the National Science Foundation; the Consortium for Nonproliferation Enabling Capabilities; the Institute for Basic Science (Korea, grant no. IBS-R017-G1-2019-a00); the Ministry of Science and Higher Education of the Russian Federation (Project "Fundamental properties of elementary particles and cosmology" No. 0723-2020-0041); the Russian Foundation for Basic Research (Project 20-02-00670_a); and the US DOE Office of Science Graduate Student Research (SCGSR) program, administered for DOE by the Oak Ridge Institute for Science and Education which is in turn managed by Oak Ridge Associated Universities. Sandia National Laboratories is a multi-mission laboratory managed and operated by National Technology and Engineering Solutions of Sandia LLC, a wholly owned subsidiary of Honeywell International Inc., for the U.S. Department of Energy's National Nuclear Security Administration under contract DE-NA0003525. The Triangle Universities Nuclear Laboratory is supported by the U.S. Department of Energy under grant DE-FG02-97ER41033. Laboratory Directed Research and Development funds from Oak Ridge National Laboratory also supported this project. This research used the Oak Ridge Leadership Computing Facility, which is a DOE Office of Science User Facility.

References

[1] D. Z. Freedman. "Coherent Neutrino Nucleus Scattering as a Probe of the Weak Neutral Current." *Phys. Rev. D* **9**, 1389–1392 (1974).

[2] V. B. Kopeliovich and L. L. Frankfurt. "Isotopic and chiral structure of neutral current." *JETP Lett.* **19**, 145–147 (1974).

[3] D. Akimov et al. (COHERENT). "Observation of Coherent Elastic Neutrino-Nucleus Scattering." *Science* **357**, 1123–1126 (2017). 1708.01294.

[4] D. Akimov et al. (COHERENT). "First Measurement of Coherent Elastic Neutrino-Nucleus Scattering on Argon." *Phys. Rev. Lett.* **126**, 012002 (2021). 2003.10630.

[5] J. Barranco, O. G. Miranda, and T. I. Rashba. "Probing new physics with coherent neutrino scattering off nuclei." *JHEP* **12**, 021 (2005). hep-ph/0508299.

[6] P. Vogel and J. Engel. "Neutrino Electromagnetic Form-Factors." *Phys. Rev. D* **39**, 3378 (1989).

[7] A. C. Dodd, E. Papageorgiu, and S. Ranfone. "The Effect of a neutrino magnetic moment on nuclear excitation processes." *Phys. Lett. B* **266**, 434–438 (1991).

[8] K. Scholberg. "Prospects for measuring coherent neutrino-nucleus elastic scattering at a stopped-pion neutrino source." *Phys. Rev. D* **73**, 033005 (2006). hep-ex/0511042.

[9] T. S. Kosmas, O. G. Miranda, D. K. Papoulias, M. Tortola, and J. W. F. Valle. "Probing neutrino magnetic moments at the Spallation Neutron Source facility." *Phys. Rev. D* **92**, 013011 (2015). 1505.03202.

[10] J. Papavassiliou, J. Bernabeu, and M. Passera. "Neutrino-nuclear coherent scattering and the effective neutrino charge radius." *PoS* **HEP2005**, 192 (2006). hep-ph/0512029.

[11] M. Cadeddu, C. Giunti, K. A. Kouzakov, Y. F. Li, A. I. Studenikin, and Y. Y. Zhang. "Neutrino Charge Radii from COHERENT Elastic Neutrino-Nucleus Scattering." *Phys. Rev. D* **98**, 113010 (2018). [Erratum: Phys.Rev.D 101, 059902 (2020)], 1810.05606.

[12] J. A. Formaggio, E. Figueroa-Feliciano, and A. J. Anderson. "Sterile Neutrinos, Coherent Scattering and Oscillometry Measurements with Low-temperature Bolometers." *Phys. Rev. D* **85**, 013009 (2012). 1107.3512.

[13] A. J. Anderson, J. M. Conrad, E. Figueroa-Feliciano, C. Ignarra, G. Karagiorgi, K. Scholberg, M. H. Shaevitz, and J. Spitz. "Measuring Active-to-Sterile Neutrino Oscillations with Neutral Current Coherent Neutrino-Nucleus Scattering." *Phys. Rev. D* **86**, 013004 (2012). 1201.3805.

[14] J. Barranco, O. G. Miranda, and T. I. Rashba. "Probing new physics with coherent neutrino scattering off nuclei." *JHEP* **12**, 021 (2005). hep-ph/0508299.

[15] B. Dutta, R. Mahapatra, L. E. Strigari, and J. W. Walker. "Sensitivity to Z-prime and nonstandard neutrino interactions from ultralow threshold neutrino-nucleus coherent scattering." *Phys. Rev. D* **93**, 013015 (2016). 1508.07981.

[16] O. G. Miranda, D. K. Papoulias, G. Sanchez Garcia, O. Sanders, M. Tórtola, and J. W. F. Valle. "Implications of the first detection of coherent elastic neutrino-nucleus scattering (CEvNS) with Liquid Argon." *JHEP* **05**, 130 (2020). [Erratum: JHEP 01, 067 (2021)], 2003.12050.

[17] P. Coloma, I. Esteban, M. C. Gonzalez-Garcia, and M. Maltoni. "Improved global fit to Non-Standard neutrino Interactions using COHERENT energy and timing data." *JHEP* **02**, 023 (2020). [Addendum: JHEP 12, 071 (2020)], 1911.09109.

[18] P. Coloma and T. Schwetz. "Generalized mass ordering degeneracy in neutrino oscillation experiments." *Phys. Rev. D* **94**, 055005 (2016). [Erratum: Phys.Rev.D 95, 079903 (2017)], 1604.05772.

[19] P. Coloma, P. B. Denton, M. C. Gonzalez-Garcia, M. Maltoni, and T. Schwetz. "Curtailing the Dark Side in Non-Standard Neutrino Interactions." *JHEP* **04**, 116 (2017). 1701.04828.

[20] P. Coloma, M. C. Gonzalez-Garcia, M. Maltoni, and T. Schwetz. "COHERENT Enlightenment of the Neutrino Dark Side." *Phys. Rev. D* **96**, 115007 (2017). 1708.02899.

[21] B. Dutta, R. F. Lang, S. Liao, S. Sinha, L. Strigari, and A. Thompson. "A global analysis strategy to resolve neutrino NSI degeneracies with scattering and oscillation data." *JHEP* **09**, 106 (2020). 2002.03066.

[22] B. K. Cogswell and P. Huber. "Detection of Breeding Blankets Using Antineutrinos." *Science & Global Security* **24**, 114–130 (2016).

[23] M. Cadeddu, N. Cargioli, F. Dordei, C. Giunti, Y. F. Li, E. Picciau, C. A. Ternes, and Y. Y. Zhang. "New insights into nuclear physics and weak mixing angle using electroweak probes." (2021). 2102.06153.

[24] M. Cadeddu, C. Giunti, Y. F. Li, and Y. Y. Zhang. "Average CsI neutron density distribution from COHERENT data." *Phys. Rev. Lett.* **120**, 072501 (2018). 1710.02730.

[25] P. S. Amanik and G. C. McLaughlin. "Nuclear neutron form factor from neutrino nucleus coherent elastic scattering." *J. Phys. G* **36**, 015105 (2009).

[26] K. Patton, J. Engel, G. C. McLaughlin, and N. Schunck. "Neutrino-nucleus coherent scattering as a probe of neutron density distributions." *Phys. Rev. C* **86**, 024612 (2012). 1207.0693.

[27] D. Akimov et al. (COHERENT). "COHERENT 2018 at the Spallation Neutron Source." (2018). 1803.09183.

[28] B. Abi et al. (DUNE). "Supernova Neutrino Burst Detection with the Deep Underground Neutrino Experiment." (2020). 2008.06647.

[29] B. Mosconi, P. Ricci, E. Truhlik, and P. Vogel. "Model dependence of the neutrino-deuteron disintegration cross sections at low energies." *Phys. Rev. C* **75**, 044610 (2007). nucl-th/0702073.

[30] Shung-Ichi Ando, Young-Ho Song, and Chang Ho Hyun. "Neutrino-Deuteron Reactions at Solar Neutrino Energies in Pionless Effective Field Theory with Dibaryon Fields." *Phys. Rev. C* **101**, 054001 (2020). 1911.11307.

[31] B. Acharya and S. Bacca. "Neutrino-deuteron scattering: Uncertainty quantification and new $L_{1,A}$ constraints." *Phys. Rev. C* **101**, 015505 (2020). 1911.12659.

[32] R. Rapp (COHERENT). "COHERENT Plans for D_2O at the Spallation Neutron Source." *In Meeting of the Division of Particles and Fields of the American Physical Society* (2019). 1910.00630.

[33] S. Agostinelli et al. (GEANT4). "GEANT4–a simulation toolkit." *Nucl. Instrum. Meth. A* **506**, 250–303 (2003).

[34] J. Allison et al. "Recent developments in Geant4." *Nucl. Instrum. Meth. A* **835**, 186–225 (2016).

[35] J. Allison et al. "Geant4 developments and applications." *IEEE Trans. Nucl. Sci.* **53**, 270 (2006).

[36] H. W. Bertini. "Intranuclear-cascade calculation of the secondary nucleon spectra from nucleon-nucleus interactions in the energy range 340 to 2900 mev and comparisons with experiment." *Phys. Rev.* **188**, 1711–1730 (1969).

[37] D. Pershey. "New Results from the COHERENT CsI[Na] Detector." (2020). 2020 Magnificent CEvNS Presentation, URL https://indico.cern.ch/event/943069/sessions/370765/#20201116.

[38] A. Konovalov. "COHERENT at SNS and CsI[NaI] Effort Update." (2020). 2020 Magnificent CEvNS Presentation, URL https://indico.cern.ch/event/943069/sessions/370765/#20201116.

[39] J. A. Formaggio and G. P. Zeller. "From eV to EeV: Neutrino Cross Sections Across Energy Scales." *Rev. Mod. Phys.* **84**, 1307–1341 (2012). 1305.7513.

[40] E. Pasierb, H. S. Gurr, J. Lathrop, F. Reines, and H. W. Sobel. "Detection of Weak Neutral Current Using Fission $\bar{\nu}_e$ on Deuterons." *Phys. Rev. Lett.* **43**, 96 (1979).

[41] S. E. Willis et al. "A Neutrino Experiment to Test the Nature of Muon Number Conservation." *Phys. Rev. Lett.* **44**, 522 (1980). [Erratum: Phys.Rev.Lett. 44, 903 (1980), Erratum: Phys.Rev.Lett. 45, 1370 (1980)].

[42] A. G. Vershinsky et al. "Measurement of the cross-sections for the interaction of fission anti-neutrinos with deuterons at the Rovno atomic power plant." *JETP Lett.* **53**, 513–516 (1991).

[43] S. P. Riley et al. "Neutrino induced deuteron disintegration experiment." *Phys. Rev. C* **59**, 1780–1789 (1999). hep-ex/9904001.

[44] Yu. V. Kozlov et al. "Anti-neutrino deuteron experiment at Krasnoyarsk." *Phys. Atom. Nucl.* **63**, 1016–1019 (2000). hep-ex/9912047.

[45] Yu. V. Kozlov et al. "A neutrino induced deuteron disintegration experiment at the Krasnoyarsk nuclear reactor." *Nucl. Phys. B Proc. Suppl.* **110**, 414–416 (2002).

[46] E. G. Adelberger et al. "Solar fusion cross sections II: the pp chain and CNO cycles." *Rev. Mod. Phys.* **83**, 195 (2011). 1004.2318.

[47] J. Carlson, D. O. Riska, R. Schiavilla, and Robert B. Wiringa. "Weak proton capture reactions on 1H and 3He and tritium 2-beta decay." *Phys. Rev. C* **44**, 619–625 (1991).

[48] K. Abe et al. (Super-Kamiokande). "Atmospheric neutrino oscillation analysis with external constraints in Super-Kamiokande I-IV." *Phys. Rev. D* **97**, 072001 (2018). 1710.09126.

[49] K. Abe et al. (Hyper-Kamiokande). "Hyper-Kamiokande Design Report." (2018). 1805.04163.

[50] W. Bugg, Yu. Efremenko, and S. Vasilyev. "Large Plastic Scintillator Panels with WLS Fiber Readout; Optimization of Components." *Nucl. Instrum. Meth. A* **758**, 91–96 (2014). 1312.0997.

[51] L. Michel. "Interaction between four half spin particles and the decay of the μ meson." *Proc. Phys. Soc. A* **63**, 514–531 (1950).

[52] J. R. Musser et al. (TWIST). "Measurement of the Michel parameter rho in muon decay." *Phys. Rev. Lett.* **94**, 101805 (2005). hep-ex/0409063.

[53] M. Janecek. "Reflectivity Spectra for Commonly Used Reflectors." *IEEE Transactions on Nuclear Science* **59**, 490–497 (2012).

[54] Hamamatsu Photonics K.K. *Large Photocathode Area Photomultiplier Tubes* (2020). URL https://www.hamamatsu.com/resources/pdf/etd/LARGE_AREA_PMT_TPMH1376E.pdf.

[55] S. Das. "A simple alternative to the Crystal Ball function." (2016). 1603.08591.

[56] S. Nakamura et al. "Neutrino deuteron reactions at solar neutrino energies." *Nucl. Phys. A* **707**, 561–576 (2002). nucl-th/0201062.

[57] S. Nakamura et al. "Tables of Neutrino (Anti-Neutrino) Deuteron Reactions Cross Sections." http://boson.physics.sc.edu/~gudkov/NU-D-NSGK/Netal/index.html. Accessed Feb. 16 2021.

[58] D. Akimov et al. (COHERENT). "First Constraint on Coherent Elastic Neutrino-Nucleus Scattering in Argon." *Phys. Rev. D* **100**, 115020 (2019). 1909.05913.

[59] C. Roecker, A. Bernstein, N. S. Bowden, B. Cabrera-Palmer, S. Dazeley, M. Gerling, P. Marleau, M. D. Sweany, and K. Vetter. "Design of a transportable high efficiency fast neutron spectrometer." *Nucl. Instrum. Meth. A* **826**, 21–30 (2016).

[60] J. Albert *et al.* "SNOwGLoBES: SuperNova Observatories with GLoBES." (2018). URL https://github.com/SNOwGLoBES/snowglobes/blob/master/doc/snowglobes_1.2.pdf.

[61] W. C. Haxton. "Neutrino Reactions on Oxygen and a Proposed Measurement of the Weinberg Angle." *Phys. Rev. C* **37**, 2660–2664 (1988).

[62] K. Langanke, P. Vogel, and E. Kolbe. "Signal for supernova muon-neutrino and tau-neutrino neutrinos in water Cherenkov detectors." *Phys. Rev. Lett.* **76**, 2629–2632 (1996). nucl-th/9511032.

[63] L. B. Auerbach et al. (LSND). "Measurements of charged current reactions of nu(e) on 12-C." *Phys. Rev. C* **64**, 065501 (2001). hep-ex/0105068.

[64] B Armbruster et al. (KARMEN). "Measurement of the weak neutral current excitation C-12(nu(mu) nu'(mu))C*-12(1+,1,15.1-MeV) at E(nu(mu)) = 29.8-MeV." *Phys. Lett. B* **423**, 15–20 (1998).

[65] C. Hagmann, D. Lange, and D. Wright. "Cosmic-ray shower generator (CRY) for Monte Carlo transport codes." *In 2007 IEEE Nuclear Science Symposium Conference Record*, volume 2, pp. 1143–1146 (2007).

[66] S. Sakakibara and L. M. Sehgal. "Corrections to Electron-neutrino Muon-neutrino Universality in Neutral Current Interactions." *Phys. Lett. B* **83**, 77–79 (1979).

[67] L. M. Sehgal. "Differences in the Coherent Interactions of ν_e, ν_μ and ν_τ." *Phys. Lett. B* **162**, 370–372 (1985).

[68] O. Tomalak, P. Machado, V. Pandey, and R. Plestid. "Flavor-dependent radiative corrections in coherent elastic neutrino-nucleus scattering." *JHEP* **02**, 097 (2021). 2011.05960.

[69] J.D. Galambos et al. "Final Design Report Proton Power Upgrade Project." (2020). URL https://neutrons.ornl.gov/sites/default/files/Final_Design_Report.pdf.

[70] J.D. Galambos et al. "Technical Design Report, Second Target Station." (2015). URL https://www.osti.gov/biblio/1185891.